FICTITIOUS CRACK MODELS : A CLASSIFICATION APPROACH

S. Weihe and B. Kröplin
Institute for Statics and Dynamics of Aerospace Structures,
University of Stuttgart, Germany

Abstract

The heuristic considerations, which are responsible for the orientation of the fictitious cracks in the classical models, are replaced by an analytically derived expression. The critical directions of the failure planes are shown to depend solely on the character of the unilateral fracture criterion and on the applied loading. The ductility of the material is found to play a key role in the process of secondary cracking. Based on these findings, the range of applicability of the classical formulations is assessed. The analytical model also allows for the derivation of a homogenized 'equivalent macroscopic failure criterion', which can be related directly to Griffith's criterion of fracture mechanics.

1 Introduction

Concrete exhibits an immense variety of failure mechanisms. It is therefore not astonishing that a wealth of different methodologies is used to describe these phenomena. Cracking of large structures is successfully ana-

lyzed using three-dimensional Fracture Mechanics. The combined crushing and cracking failure of triaxially loaded laboratory specimens is well represented by phenomenological models which are based on anisotropic damage and plasticity. The transition between the small laboratory scale and the scale of large concrete structures is accomplished by non-local approaches which properly account for the size effect.

The ability to reliably predict the nonlinear behaviour of concrete, or any other material, demands a sound calibration of the constitutive models. However, even more important is the requirement that the applied load history remains within the range of applicability of the material model. Phenomenological models - in a broad sense - interpolate the accumulated response of all active nonlinearities. This implies that the calibration procedure must reflect the interaction properly. If the load history of the structure does activate a different combination of failure mechanisms, the prediction might be quite inapplicable – and in the most cases, there is no 'warning flag' which would indicate this.

An alternative philosophy of designing constitutive models is to identify the dominant types of failure and to model their specific response individually. Unfortunately, an abundance of mechanisms may exist, as is the case for concrete. The advantage of such models is that the material parameters have a clear physical relevance and that an appropriate calibration procedure can be devised. The range of applicability is given by the occurrence of the failure modes, i.e. if the constitutive model includes all mechanisms which are active during the load history, then the numerical simulation should give reliable predictions.

These might be some of the reasons for the widespread use of Fictitious Crack Models. Following the original work of Rashid (1968), the terminus technicus has been coined by Hillerborg et al. (1976) in their inspiring contribution: The crack is not realized as a topological discontinuity but rather through its constitutive consequences across the ligament. The sudden drop in strength and/or stiffness across the crack is replaced by a continuous degradation, not only for numerical reasons but also to avoid the singularity at the crack tip in the spirit of Dugdale and Barrenblatts work. This renders the approach mesh objective, as has been demonstrated by Bažant & Oh (1983). The formation of cracks is accompanied by a stress redistribution, which can cause the occurrence of shear stresses across the process zone. Even if the failure has been initiated under pure Mode I conditions, complex mixed mode situations may arise during the failure process. They have to be accounted for by mode separation techniques.

The stress redistribution (as well as the application of different load cases) causes a rotation of the principal loading directions. The various classical

Fictitious Crack Models react to such a rotation in an inherently very different manner. Thus, they do not converge to a common solution, and the qualitative differences are unsurmountable. Nevertheless, since the physical nonlinearity is entirely determined by these oriented mechanisms, this issue is of utmost importance and should be resolved.

2 Basic ingredients

2.1 The smeared crack concept and stress consistency

The tractions $[q_n, q_t]$, which act on each fracture plane i at an (integration) point, are resolved from the global stresses through the usual projection,

$$[q_n, q_t]_i^T = \boldsymbol{N}_i^T \boldsymbol{\sigma} \tag{1}$$

where $\boldsymbol{N}$ constitute the direction cosines of the fracture plane. Thus, the local stresses in the plane are always consistent with the global stress field, i.e. any change of the stress state is reflected immediately in each failure plane.

Following the ideas of Litton (1974), the total strain rate $\dot{\varepsilon}$ is decomposed into one part of the response of the continuum $\dot{\varepsilon}^{co}$, which might include nonlinearities e.g. due to visco-plasticity or shrinkage, and the individual contributions $\dot{\varepsilon}_i^{cr}$ due to the relative crack opening and sliding displacements $[u_n, u_t]_i^{cr}$ of each crack.
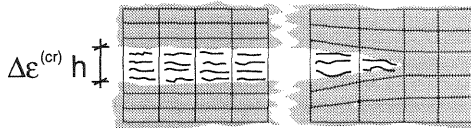

$$\dot{\varepsilon} = \dot{\varepsilon}^{co} + \sum_i \dot{\varepsilon}_i^{cr} \tag{2}$$

$$\dot{\varepsilon}_i^{cr} = \boldsymbol{N}_i \frac{1}{h} [\dot{u}_n, \dot{u}_t]_i^{cr} \tag{3}$$

Figure 1: The smeared crack

The width h of the crack band is thereby strongly related to the element size and geometry, cf. Oliver (1989).

2.2 Constitutive laws for the process zone

The constitutive law which describes the degradation of the individual failure plane is the basic ingredient of any Fictitious Crack Model. Since the redistribution of stresses and a subsequent rotation of the principal stresses and strains inevitably leads to mixed mode situations, the constitutive formalism must provide for a consistent mode separation. The following model satisfies this requirement and will be used to derive the explicit formulae in the subsequent sections without loss of generality of the arguments. Since the model itself is not subject of the present discussion, only an outline of the model is given. For a detailed description, the reader is referred to Weihe et al. (1994).
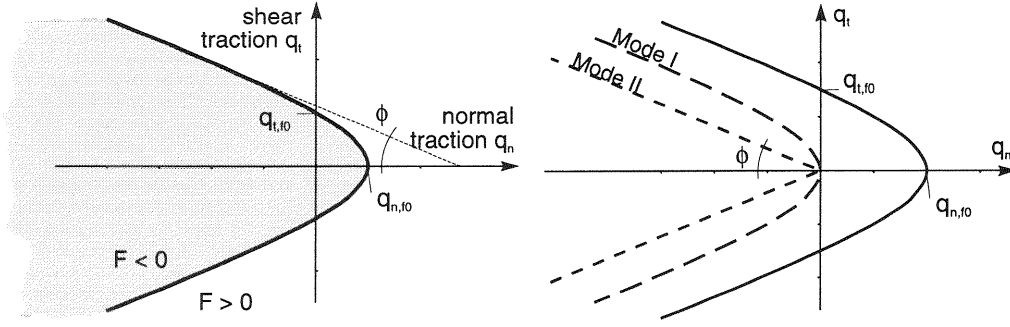
Figure 2: The fracture criterion at initial failure and its residual shapes

$$F := -q_n \left(q_n - q_{n,f0} \left(1 + \frac{\gamma^2}{\tan^2\phi} \right) \right) + \frac{q_t^2}{\tan^2\phi} - q_{n,f0}^2 \frac{\gamma^2}{\tan^2\phi} \leq 0 \qquad (4)$$

$[q_n, q_t]$ denote the current normal and tangential (shear) tractions in the failure plane, $q_{n,f0}$ and $q_{t,f0} = \gamma \cdot q_{n,f0}$ are the initial normal and shear strength of the plane. It is noted that the residual surface for Mode I failure differs from the residual surface obtained in Mode II situations (which is the Mohr-Coulomb criterion, characterized by the friction angle ϕ).

The relaxation mechanism is expressed in a pressure dependent, non-associated 'flow rule' for the inelastic crack opening and sliding displacements $[u_n^{cr}, u_t^{cr}]$.

$$\dot{u}^{cr} = \dot{\lambda}\frac{\partial G}{\partial q} := \dot{\lambda} \begin{bmatrix} \eta & 0 \\ 0 & 1 \end{bmatrix} \frac{\partial F}{\partial q} \qquad\qquad \eta := \exp\left(-q_{t,r}\eta_0\right)$$

$$F \leq 0 \quad , \quad \dot{\lambda} \geq 0 \quad , \quad F\dot{\lambda} = 0 \qquad\qquad q_{t,r} := \langle -q_n \rangle \tan\phi \qquad (5)$$

The evolution laws for the degradation are formulated with two independent energy state variables ξ, which equilibrate the critical energy release rates G_f^I and G_f^{II} after complete debonding and ensure objectivity with respect to mesh refinement.

$$\dot{\xi}^I \quad := \quad \begin{cases} \frac{1}{G_f^I} q_n \dot{u}_n^{cr} & , \quad \dot{u}_n^{cr} \geq 0 \\ 0 & , \quad \dot{u}_n^{cr} < 0 \end{cases} \qquad\qquad (6)$$

$$\dot{\xi}^{II} \quad := \quad \frac{1}{G_f^{II}} \| \left(\|q_t\| - q_{t,r} \right) \dot{u}_t^{cr} \| \qquad\qquad (7)$$

2.3 Classical Fictitious Crack Models

The orientation of the failure planes becomes a decisive property of the Fictitious Crack Models. The classical formulations, i.e. the Fixed Crack and
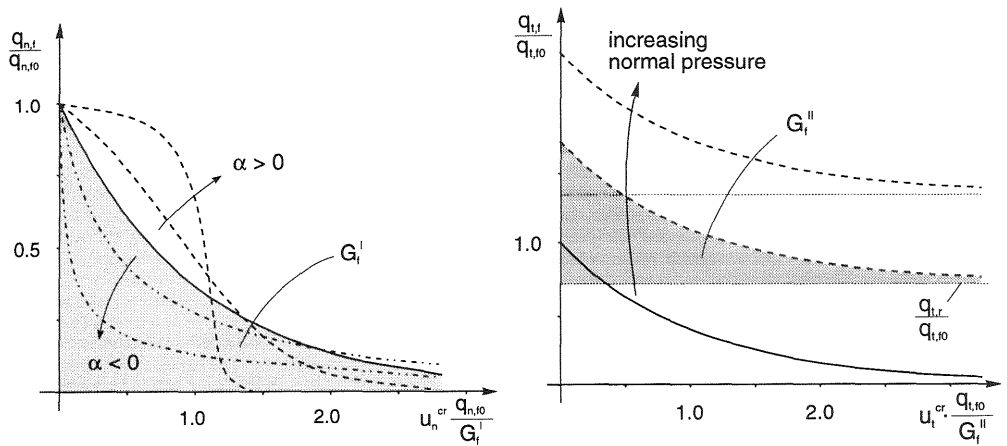
Figure 3: The degradation of the normal strength (Mode I) and the shear strength (Mode II, different compressive normal loads applied)

Rotating Crack Model with their more advanced successors in the form of the Multiple Fixed Crack or (statically constrained) Microplane Model, will now be reviewed in that context, cf. Carol & Prat (1991), Rots (1988), and Willam et al. (1987).

In the Fixed Crack Model, the crack is initiated perpendicular to the maximum tensile (principal) stress when this stress exceeds the tensile strength $q_{n,f0}$ of the material. Secondary cracking is not accounted for, and thus non-proportional loading can result in stresses parallel to the initial crack which may exceed the uniaxial strength by far. The Rotating Crack Model resolves this situation by adjusting the failure mechanism (i.e. the material anisotropy) to the current loading state and thus monitoring only (locally uniaxial) Mode I stress states. Consequently, the degradation mechanism is controlled by the major principal stress only. The Multiple Fixed Crack Concept retains the physical plausibility of the Fixed Crack approach, but it allows for secondary cracking if the inclination of the principal stresses against existing cracks exceeds a threshold value α^{Th}. However, the crack is initiated in Mode I and the choice of the threshold angle remains arbitrary.

A different concept is pursued by the Microplane Model with a static constraint. The potential crack planes are predefined in the sense (of an arbitrary number) of sample directions. The degrading mechanism is initiated whenever the local fracture criterion F is violated (which does not necessarily need to occur under local Mode I conditions!). Secondary cracking is thus incorporated naturally.

As demonstrated, the two issues which constitute the main interest in this context, namely the orientation of the primary crack and especially the re-

sponse to non-proportional loading which may induce secondary cracking, are treated with fundamentally different approaches.

3 The critical crack direction

The material is assumed to be homogeneous and isotropic in the initial undamaged state and thus the fracture criterion F_0 with the virgin material characteristics $q_{n,f0}$, $q_{t,f0}$ and ϕ is valid for any newly formed crack plane. The second assumption, which is closely correlated to the first one, states that the material degradation due to crack formation is confined to the individual crack plane, i.e. the angular neighbourhood is not affected. Thus a crack is initiated if and only if the tractions in a plane with critical orientation α_{crit} reach a critical value $[\hat{q}_n, \hat{q}_t]$ and activate the fracture criterion F_0.

The locally applied tractions are given in dependence of the macroscopic (principal) stress state $[\sigma_I, \sigma_{II}]$ by the well-known transformation rules due to Mohr (see eqn.(1)):

$$q_n = \sigma_I \cos^2\alpha + \sigma_{II} \sin^2\alpha \quad , \quad q_t = \frac{\sigma_I - \sigma_{II}}{2} \sin(2\alpha) \qquad (8)$$

The evolution of the stresses from the current to a critical state is determined by the applied loading and the nonlinear response of the structure to it. The stress history is assumed to be linear inside a time step. For proportional loading in the elastic range, as well as for small time steps inside the nonlinear regime, the assumption of a proportional increment yields a constant value of the load-type parameter ζ.

$$\zeta := \frac{\sigma_I + \sigma_{II}}{\sigma_I - \sigma_{II}} \overset{!}{=} \frac{\hat{\sigma}_I + \hat{\sigma}_{II}}{\hat{\sigma}_I - \hat{\sigma}_{II}} =: \hat{\zeta} \qquad (9)$$

The following special cases of ζ are readily verified:

$-\infty$	-1	0	$+1$	$+\infty$
hydr. compr.	uniax. compr.	pure shear	uniax. tension	hydr. expansion

Now all necessary ingredients to uniquely identify the orientation of the critical plane are given: The expression for the load-type parameter ζ yields the transition between the current and the critical loading state. Substituting it into eqn.(8) and introducing the expression obtained for the critical tractions into the fracture criterion in general yields an expression of the following format:

$$F(\zeta, \alpha) \leq 0 \quad , \quad \alpha_{crit} = \left\{ \alpha \, \middle| \, F(\zeta, \alpha) \overset{!}{=} \max \right\} \qquad (10)$$
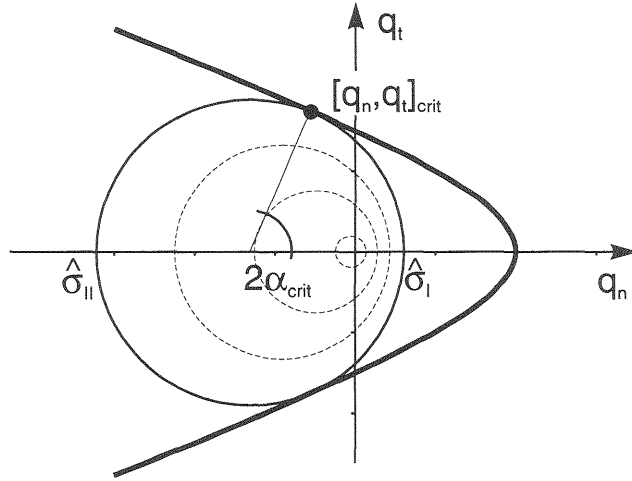
Figure 4: The critical direction α_{crit}

The critical direction α_{crit} maximizes the left hand side of eqn.(10). For the hyperbolic fracture criterion given in (4), the condition for fracture initiation ($F = 0$) can be finally written as

$$\cos(2\alpha_{crit}) = \frac{\frac{\tan^2\phi\ \zeta}{(1+\tan^2\phi)(\gamma^2+\tan^2\phi)}\sqrt{\left(1+\tan^2\phi\right)\left(4\gamma^2-\left(1-\zeta^2\right)\left(\gamma^2-\tan^2\phi\right)^2\right)}-1}{\zeta-\frac{1}{\gamma^2+\tan^2\phi}\sqrt{\left(1+\tan^2\phi\right)\left(4\gamma^2-\left(1-\zeta^2\right)\left(\gamma^2-\tan^2\phi\right)^2\right)}} \tag{11}$$

It is seen that the critical direction depends only on the character of the local fracture criterion (γ, ϕ) and the applied loading ζ. Since this approach can be applied to any fracture criterion, the critical direction can be expressed for any unilateral fracture criterion F in the following format:

$$\alpha_{crit} = \alpha_{crit}\left(\zeta\right) \quad \text{for a given material.} \tag{12}$$

For complex fracture criteria or a general relationship between the current and the critical load-type parameter, the corresponding expression for the critical angle α_{crit} may have to be solved for numerically.

3.1 Is fracture initiation under Mode I applicable?
The angle α between the principal stress and the normal to the fracture plane is synonymous with the determination of the failure mode. Thus, the condition for failure under Mode I is derived (cf. Fig. 5) from eqn.(11).

$$\alpha_{crit} = 0° \quad \Longleftrightarrow \quad 0 \leq 1 - \frac{\zeta-1}{\zeta+1} \leq \gamma^2 - \tan^2\phi \tag{13}$$
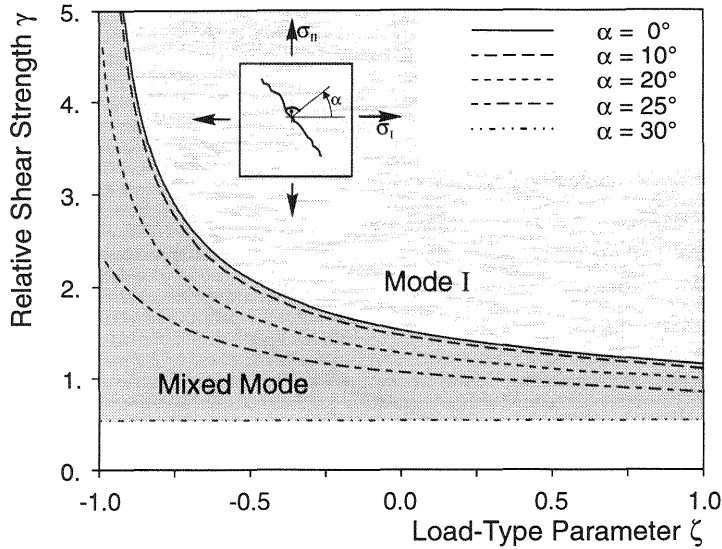
831

Figure 5: Transition between failure modes ($\phi = 30°$)

Again, the important parameters are the load-type (left part) and the material characteristics (right part of the inequality). It is found that:

o Mode I failure is feasible for $\zeta \geq -1$. Even a macroscopic stress state of pure shear may lead to local Mode I fracture.

o If the applied loading is dominated by tensile components, then failure under Mode I is favoured. For pure equibiaxial tension, failure necessarily occurs under Mode I.

o Materials with a low relative shear strength $\gamma := q_{t,f0}/q_{n,f0}$ usually fail under mixed mode ($\rightsquigarrow$ metals, polymers), whereas materials with a high relative shear strength tend to fail under Mode I ($\rightsquigarrow$ concrete, ceramics).

In conclusion, cracks will occur under Mode I if the material is sufficiently brittle *and* if the loading is dominated by tensile components. In other cases, such as in the neighbourhood of loading platens, the maximum stress criterion for fracture initiation is inadequate.

3.2 Orientation of secondary cracks

The most important finding of the previous section is, however, that eqn.(11) is not only valid for the initiation of the primary crack, but, due to the consistency of the stresses (see above), for all subsequent cracking events as well. The 'tension-shear' problem, originally proposed by Willam et al. (1987), is used to demonstrate this important feature.

The primary crack in the tension-shear specimen is initiated through uniaxial loading under displacement control. Subsequently, the loading is ap-

832

plied with a continuous rotation of the directions of the principal strains $(\dot{\epsilon}_{xx} : \dot{\epsilon}_{yy} : 2\dot{\epsilon}_{xy} = 0.50 : 0.75 : 1.00)$.

plane stress:

$$
\begin{aligned}
E &= 10.0 \text{ GPa} \\
\nu &= 0.2 \\
\sigma_{n,f} &= 1.00 \text{ MPa} \\
\sigma_{t,f} &= 1.25 \text{ MPa} \\
\phi &= 20^o \\
G_f^I &= 0.15 \text{ J/m}^2 \\
G_f^{II} &= 0.20 \text{ J/m}^2
\end{aligned}
$$

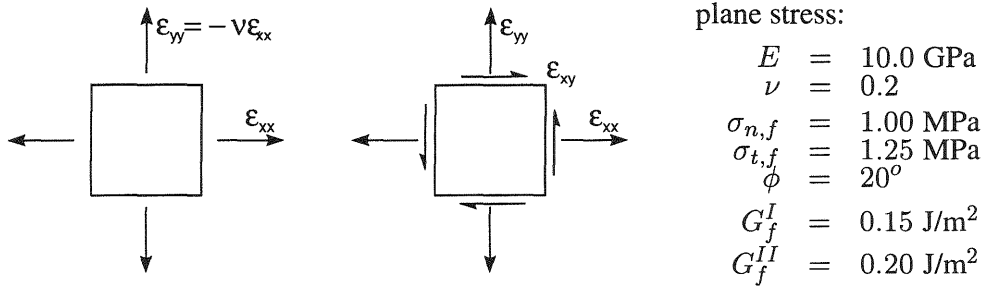Figure 6: Tension-Shear: Loading (a) before and (b) after initial failure

It is clearly seen from Fig. 7 that even for identical material parameters, the characteristic response differs drastically for the conventional models, cf. Willam et al. (1987), Rots (1988), and Feenstra (1993). Since these differences are caused by the fundamentally different assumptions inherent in the model, the various results do not converge to a common solution – and thus the computational predictions are difficult to assess.
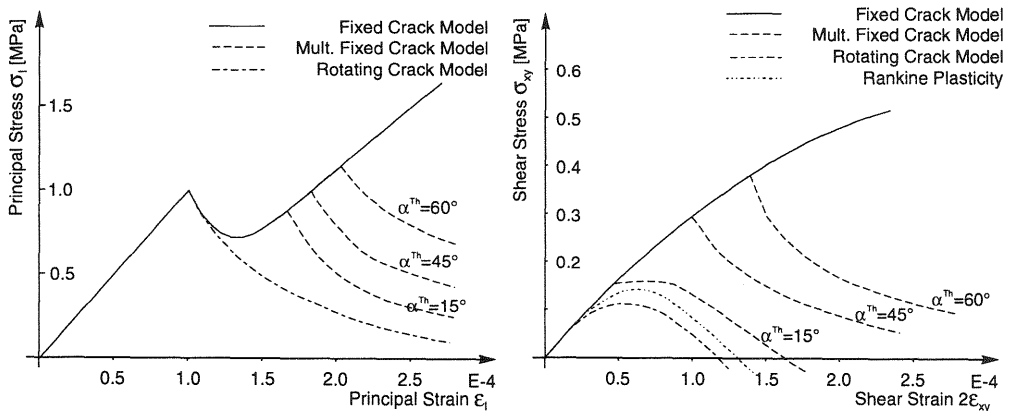

Figure 7: 'Tension-Shear' problem: Conventional Models

With the present approach, the formation of secondary cracks is uniquely defined by an analytical derivation ($\rightsquigarrow$ eqn.(11)) that replaces the variety of heuristic assumptions addressed in section 2.3. The results become objective. As shown in Fig. 8, the ductility of the material has a significant influence on the angle between primary and secondary (and further) crack(s). Therefore, the material dependent relative toughness $\mathcal{Z}$ is introduced. It correlates the potential energy, which is stored in the material at the instant of

Figure 8: Material dependent initiation of secondary cracking
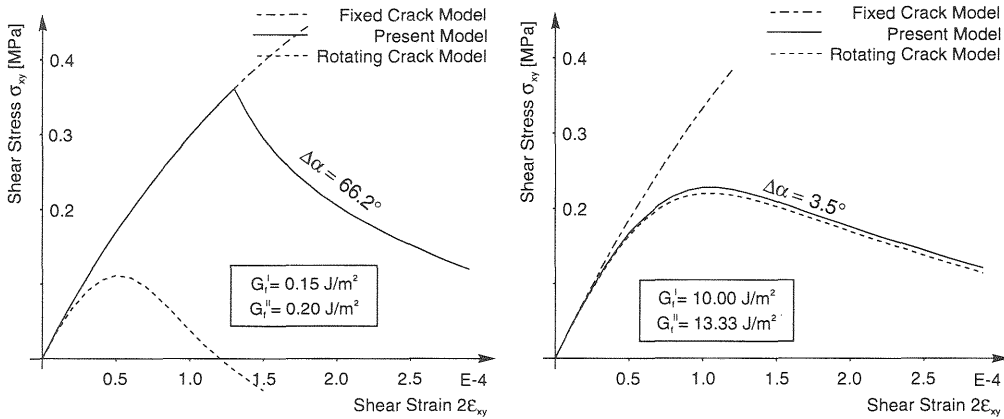
○ Brittle materials are characterized by a very pronounced softening after crack initiation. Stresses perpendicular to the ligament are relaxed and further cracking is shielded against. Therefore, the applied stress state must rotate significantly before secondary cracking can occur.

○ Ductile materials do not exhibit an abrupt loss of strength, the stress relaxation is not pronounced. Hence, the critical stress state can be exceeded in the neighbourhood of the initial crack as well and secondary failure can occur at only a slight inclination to the primary 'crack'.

failure initiation (failure is triggered by a strength criterion!), and the dissipated energy during failure. $\mathcal{Z}$ has the dimensions of length and has previously been interpreted as a characteristic length parameter.

$$\mathcal{Z} := \frac{E}{1 - \nu^2} \cdot \frac{G_f^I}{q_{n,f0}^2} \tag{14}$$

However, the interpretation in terms of energies explains the essence of Fig. 9: If the potential energy at failure initiation is sufficient to instantaneously form the free crack surface ($\leadsto$ brittle material), then the sudden stress relief activates extensive crack shielding, and secondary cracking can occur only perpendicular to the primary crack. An associated flow rule mobilizes additional stresses due to dilatancy effects, which leads to a premature secondary cracking. On the other hand, ductile materials ($\mathcal{Z} \gg 1$) do not relieve stresses and consequently do not activate crack shielding. Thus, the rotating applied stresses violate all failure planes subsequently in the sense of a Rotating Crack Model ($\leadsto \Delta\alpha \to 0$).

It is noted that in (perfect) plasticity and in fracture mechanics, only one single material parameter is needed to describe the failure process, which is the yield limit σ_Y and the fracture toughness G_f respectively. In the present
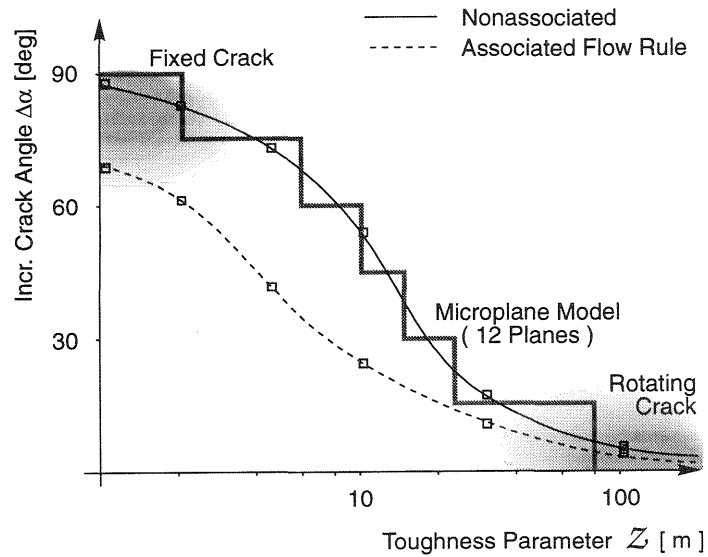
834

Figure 9: Angle $\Delta\alpha$ between primary and secondary crack in the 'Tension-Shear' problem: Predictions by the present approach and comparison with the classical models

approach, both quantities are utilized and the relative toughness $\mathcal{Z}$ establishes the correlation between them.

4 Range of applicability for the classical models

With the derived criteria, the heuristic assumptions of the conventional models can be reassessed. If a significant rotation of the principal directions of the applied loading is to be expected, the following recommendations for the range of applicability of the conventional models are deduced:

1. The Fixed, Multiple Fixed and Rotating Crack Model assume crack initiation under Mode I. This has been shown to be a valid assumption for materials with a high relative shear strength γ under tensile loading situations (eqn.(13)). Such materials typically exhibit a relatively brittle failure behaviour (e.g. concrete or ceramics).

2. As demonstrated, the inclination between primary and secondary cracking is substantial for brittle failure, because pronounced unloading and substantial shielding of cracks parallel to existing ones occurs. Since the Fixed Crack Concept does not account for secondary cracking, the Multiple Fixed Crack Model with $\alpha^{Th} \geq 45°$ should be preferred in these situations. However, the choice of α^{Th} remains arbitrary and the results should be assessed carefully.

3. The Rotating Crack Concept combines a mechanism for brittle materials (primary crack initiation under Mode I) with a concept that is appropriate for a very ductile material (continuous rotation of the material anisotropy). This is considered a major inconsistency since for quasi-brittle materials, a significant shielding of cracks must be expected. The Rotating Crack concept, as well as plasticity based formulations (e.g. Rankine) should therefore be used with care when simulating failure processes in quasi-brittle materials.

4. The statically constrained Microplane Model accounts for a proper inter-action of normal and shear components. However, a strong dependence of the results on the number of sampling directions is observed, especially if the material is not perfectly brittle but exhibits some significant tough-ness. The results converge to the analytical solution given by eqn.(11) as the number of sample directions is increased. For this case, however, the numerical treatment is very inefficient and the determination of the active set of cracks becomes extremely difficult.

The proposed Fictitious Crack Model yields consistent results for primary and secondary cracking in the complete range of materials, from perfectly brittle to ductile behaviour. Except for highly ductile materials, where classical plasticity is to be preferred for numerical reasons, the present approach is an attractive enhancement to the conventional Fictitious Crack Models.

5 Equivalent macroscopic failure criterion

5.1 Homogenization

The result for the orientation of the critical fracture plane (11) is introduced into eqn.(8). Thus the local tractions $[q_n, q_t]$ in the fracture criterion (4) can be substituted by the applied principal stresses $[\sigma_I, \sigma_{II}]$. After some calculus, the obtained equivalent macroscopic failure criterion reads:

$$
\mathcal{F} := \begin{cases} \sigma_I - q_{n,f0} \overset{!}{=} 0 \\ \text{for} \quad \sigma_I \left(\gamma^2 - \left(1 + \tan^2\phi \right) \right) + \sigma_{II} \geq 0 \\ \\ \left(\sigma_I - \sigma_{II} \right) B - q_{n,f0} \left(\left(\tan^2\phi + \gamma^2 \right) \frac{\sigma_I + \sigma_{II}}{\sigma_I - \sigma_{II}} + \sqrt{A} \right) \overset{!}{=} 0 \\ \text{for} \quad \sigma_I \left(\gamma^2 - \left(1 + \tan^2\phi \right) \right) + \sigma_{II} < 0 \end{cases}
$$

$$\tag{15}$$

with

$$A = \left(\tan^2\phi + 1\right)\left(\left(\tan^2\phi - \gamma^2\right)^2\left(\frac{(\sigma_I + \sigma_{II})^2}{(\sigma_I - \sigma_{II})^2} - 1\right) + 4\gamma^2\right)$$

$$B = \tan^2\phi\left(\frac{(\sigma_I + \sigma_{II})^2}{(\sigma_I - \sigma_{II})^2} - 1\right) - 1$$

The uniaxial tensile strength f_t' and uniaxial compressive strength f_c' are given by

$$f_t' = \begin{cases} q_{n,f0} & \text{for} \quad \gamma^2 \geq 1 + \tan^2\phi \\ q_{n,f0}\left(1 - \left(\gamma - \sqrt{1 + \tan^2\phi}\right)^2\right) & \text{for} \quad \gamma^2 < 1 + \tan^2\phi \end{cases}$$

$$f_c' = q_{n,f0}\left(1 - \left(\gamma + \sqrt{1 + \tan^2\phi}\right)^2\right) \tag{16}$$

This is in accordance with the results in section 3.1, where the tensile strength of the fracture plane could be utilized under uniaxial loading only if $\gamma^2 \geq 1 + \tan^2\phi$. Otherwise, mixed mode failure in an inclined fracture plane is predicted for uniaxial tension.

As shown in Fig. 10, the predictions for plain concrete under biaxial stresses are quite adequate in the tensile and tensile-compressive regime. The transition between failure under Mode I and mixed mode failure for increasing compressive components is captured very well. The failure in the compression regime is dominated by tensile splitting. Since the present approach has been implemented two-dimensionally, this physical failure mode, which resides in the third dimension, cannot be represented by the numerical prediction.

It should be noted that the macroscopic failure criterion and the (microscopical) Fictitious Crack Model are only equivalent at the onset of initial failure. The further evolution of the failure process is formulated in terms of micromechanically oriented fracture. This leads to a highly anisotropic softening behaviour on the equivalent macroscopic scale, which cannot be represented with homogenized quantities. Therefore, the microscopic formulation with the pertinent evolution laws should be favoured.

5.2 Correlation with Griffith's criterion

The equivalent macroscopic fracture criterion is now evaluated for a special choice of the material parameters ($\phi = 0, \gamma = 2$). The critical orientation
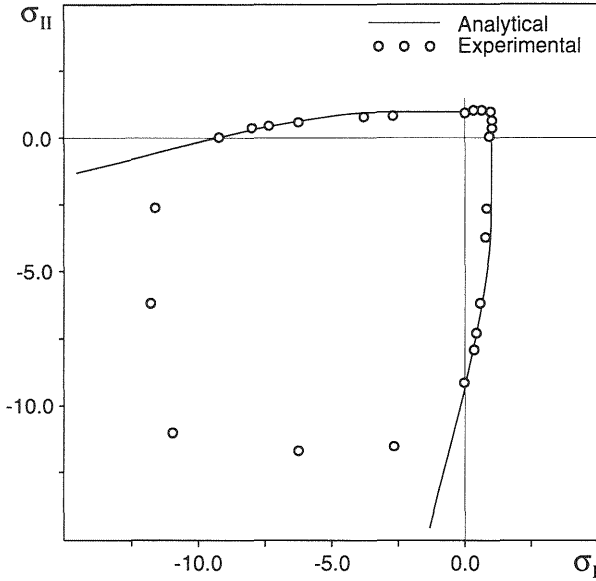
Figure 10: Comparison of the numerical predictions and experimental results after Kupfer et al. (1969)

and the fracture criterion simplify to

$$
\begin{aligned}
\cos\left(2\alpha_{crit}\right) &= 1 & \text{for} && 3\sigma_I + \sigma_{II} \geq 0 \\
\cos\left(2\alpha_{crit}\right) &= -\frac{1}{2\zeta} & \text{for} && 3\sigma_I + \sigma_{II} < 0
\end{aligned}
\tag{17}
$$

$$
\mathcal{F}_G := \begin{cases}
\sigma_I - q_{n,f0} \overset{!}{=} 0 & \text{for} & 3\sigma_I + \sigma_{II} \geq 0 \\
\left(\sigma_I - \sigma_{II}\right)^2 + 8\,q_{n,f0}\left(\sigma_I + \sigma_{II}\right) \overset{!}{=} 0 & \text{for} & 3\sigma_I + \sigma_{II} < 0
\end{cases}
$$

This criterion is syntactically identical to the fracture criterion, which Griffith (1924) derived on the basis of Inglis' solution for the stress distribution around a crack in a linear elastic continuum under plane stress conditions. However, the tensile strength $q_{n,f0}$ in Griffith's derivation is not at all a material parameter, but - as is well known from fracture mechanics - is dependent on the length a of the crack:

$$
\begin{aligned}
\text{Strength Criterion:} &\quad q_{n,f0} = \text{const} \\
\text{Fracture Mechanics:} &\quad q_{n,f0} = \sqrt{\frac{E\,G_f}{\pi a}}
\end{aligned}
\tag{18}
$$

Under the assumption that a technical material contains initial microscopical defects, and that the geometry and size of these defects is determined by the production process of the material, then the length a of the initial defects becomes a characteristic constant, and the tensile strength $q_{n,f0}$ becomes a

838

material parameter. This is the well-accepted argument for the applicability of a strength criterion to fracture initiation of a (macroscopically) undamaged material.

This argument holds as long as the crack remains 'small'. As the crack length increases, eqn.(18) becomes more and more significant and an energy controlled fracture criterion should be employed. This transition in the sense of the 'size-effect' has been applied very impressively by Swenson & Igraffea (1991).

6 Summary and conclusions

A constitutive description of the planar cracking/sliding mechanism has been presented, which includes independent softening laws for the normal and shear strength. It allows for a consistent calibration with respect to Mode I and Mode II failure and ensures a proper treatment of complex mixed mode situation.

The analytical *a priori* determination of the orientation of the crack plane yields a unique criterion for the initiation of primary and secondary cracking. It has been emphasized that cracks do not necessarily occur under Mode I conditions, and that the crack orientation is entirely defined by the characteristic strength parameters of the material and the type of the applied loading. The inclination between subsequent cracks is highly dependent on the ratio of the potential energy present in the specimen at failure initiation and the fracture toughness.

With the derived criteria, the heuristic assumptions of the conventional models have been reassessed: The Fixed Crack and Rotating Crack Model are based on very restrictive assumptions and should be applied with care. The static Microplane and the Multiple Fixed Crack Model (if $\Delta\alpha^{Th}$ is based on the relative toughness $\mathcal{Z}$ (Fig. 9)) reflect the analytical solution better. However, the present approach, which is based directly on the analytical solution for the critical plane of failure, has proven to be numerically more efficient and stable than the Microplane Approach.

The failure criterion is in good agreement with experimental results for failure initiation. Its homogenized format is identical to Griffith's criterion of fracture mechanics. However, the strength parameter has to be interpreted in the sense of the 'size-effect'. This exactly is the challenge for non-local material descriptions, which are currently under development.

7 References

Bažant, Z.P. and Oh, B.H. (1983) Crack band theory for fracture of concrete, in **Materials and Structures (RILEM, Paris)**, 16(93), 155–177.

Carol, I. and Prat, P.C. (1991) Smeared analysis of concrete fracture using a microplane based multicrack model with static constraint, in **Fracture Processes in Concrete, Rock and Ceramics** (eds J.G.M. van Mier, J.G. Rots, and A. Bakker) E&FN Spon, London, Vol.2, 619–628.

Feenstra, H.P. (1993) **Computational Aspects of Biaxial Stress in Plain and Reinforced Concrete.** Doctoral Thesis, Delft University of Technology (NL).

Griffith, A.A. (1924) The theory of rupture, in **Int. 1st Congress Appl. Mech.** (eds. Biezeno and Burgers), Delft (NL), 55–63.

Hillerborg, A., Modéer, M., and Petersson, P.E. (1976) Analysis of crack formation and crack growth in concrete by means of fracture mechanics and finite elements. **Cement and Concrete Research**, 6, 773–782.

Kupfer, H, Hilsdorf, H.K., and Rusch, H. (1969) Behavior of concrete under biaxial stresses. **Proceedings American Concrete Institute**, 66(3), 656–666.

Litton, R.W. (1974) **A Contribution to the Analysis of Concrete Structures Under Cyclic Loading**. PhD Thesis, University of California, Berkeley (USA).

Oliver, J. (1989) A consistent characteristic length for smeared cracking models. **Int. J. Num. Meth. Eng.**, 28, 461–474.

Rashid, Y.R. (1968) Analysis of prestressed concrete pressure vessels. **Nucl. Engng. and Design**, 7, 334–344.

Rots, J.G. (1988) **Computational Modeling of Concrete Fracture.** Doctoral Thesis, Delft University of Technology (NL).

Swenson, D.V. and Ingraffea, A.R. (1991) The collapse of the Schoharie Creek Bridge: A case study in concrete fracture mechanics. **Int. J. Fracture**, 51, 73–92.

Weihe, S., König, M., and Kröplin, B. (1994) A treatment of mixed mode fracture in debonding. **Comp. Mat. Sc.**, 3, 254–262.

Willam, K.J., Pramono, E., and Sture, S. (1987) Fundamental issues of smeared crack models, in **SEM/RILEM Int. Conf. on Fracture of Concrete and Rock** (eds. S.P. Shah and S.E. Swartz), Houston, Texas (USA), 142–153.